JOURNAL OF MATERIALS SCIENCE 18 (1983) 1235–1243

The relationship between crystal growth behaviour and constitution in the systems $LiF–LuF_3$, $LiF–ErF_3$ and $LiF–YF_3$

I. R. HARRIS, H. SAFI, N. A. SMITH, M. ALTUNBAS
Department of Metallurgy and Materials, University of Birmingham, Birmingham, UK

B. COCKAYNE, J. G. PLANT
Royal Signals and Radar Establishment, Malvern, Worcestershire, UK

The crystal growth behaviour of $LiRF_4$-type compounds in the systems $LiF–LuF_3$, $LiF–ErF_3$ and $LiF–YF_3$, have been related to the constitution of the respective systems. Crystal growth, differential thermal analysis (DTA) and microstructural studies indicate that the phases $LiLuF_4$ and $LiErF_4$ are clearly congruent in nature which is in agreement with previous work on these compounds. Corresponding studies for the compound $LiYF_4$ are consistent with this phase being either just congruent or just syntectic (but definitely not peritectic) in character, its constitutional behaviour depending critically on the level of contamination.

1. Introduction

This paper reports growth and constitutional studies of $LiRF_4$ phases (where R = Lu, Er or Y), made to provide relevant background information to the crystal growth behaviour of the more complex α/β-LYF compounds (e.g. $LiY_{0.434}Er_{0.5}Tm_{0.055}Ho_{0.011}F_4$) which are employed as "eye-safe" lasers [1, 2].

Single crystals of the compounds $LiLuF_4$, $LiErF_4$ and $LiYF_4$ have been grown by the Czochralski technique and detailed observations have been made during the crystal growth procedure. The systems $LiF–LuF_3$, $LiF–ErF_3$ and $LiF–YF_3$ have been investigated by DTA measurements and the microstructures of the various mixtures have been examined by electron back scattering (EBS) using a scanning electron microscope (SEM). The present phase diagrams are compared with those reported earlier [3, 4] and the significant differences are discussed.

2. Materials and experimental methods

The $LiRF_4$ samples studied here were prepared from the component fluorides. The fluorides, YF_3, ErF_3 and LuF_3 were obtained as crystalline powders heat treated in anhydrous HF and supplied by Rare-Earth Products Ltd., whilst the LiF was supplied as transparent polycrystals by British Drug Houses Ltd. For single crystal growth, mixtures of LiF and RF_3 corresponding to the requisite $LiRF_4$ were first compounded and then zone refined to yield polycrystalline bars from which clear portions were selected [2, 5] for subsequent crystal growth by the Czochralski technique using procedures and high purity conditions described fully elsewhere [2]. Specimens for differential thermal analysis and microscopy were prepared directly from the component fluorides by melting within vitreous carbon crucibles under the same purified argon atmosphere and within the same stainless steel chamber used for crystal growth [2]; these melts were solidified very slowly (about $10^\circ C h^{-1}$) to ensure that equilibrium structures were produced and then cooled more rapidly (about $100^\circ C h^{-1}$) to room temperature.

Small portions (total weight about 0.01 g) of these buttons were then examined in a Linseis L62 DTA unit in conjunction with a Stanton Redcroft linear temperature programmer. The sample chamber was evacuated to a vacuum of

0022–2461/83 $03.00 + .12

approximately 6×10^{-6} torr and the measurements were carried out in purified argon (supplied by a BOC Rare Gas Purifier) at a pressure of 0.4 atmospheres. Two types of DTA thermocouple head were employed in these studies, namely Pt/Pt–Rh and Ni/Cr–Ni/Al with respective temperature resolutions of ± 2 and ± 0.5° C. The latter was used in an attempt to resolve closely spaced thermal events or to detect weak thermal reactions; one problem with this type of head is limited lifetime due to thermal ageing. Heating and cooling rates varying between 2 and 20° C per minute were employed in these investigations, the rapid cooling rates sometimes being required to detect the liquidus temperatures. Where necessary, appropriate corrections for undercooling have been made.

Three types of crucible were used in the DTA equipment, namely alumina, platinum and tantalum, all with tightly fitting lids to minimize the loss of volatile constituents. LiF–LuF_3 and LiF–ErF_3 mixtures were compatible with all three types of crucible. For LiF–YF_3 mixtures however, there was evidence of extensive wetting and reaction between the molten samples and the walls of the tantalum crucibles. This leads to a tenacious skin of material covering the crucible interior rather than the normal consolidated sample in the bottom of the crucible. Such widespread distribution of the sample can give misleading DTA profiles, hence platinum crucibles, where no wetting is evident, were used for LiF–YF_3 mixtures. These differences in behaviour clearly suggest that LiF–YF_3 mixtures are much more reactive than the other systems.

The effect of the wetting reaction on the DTA profiles of the LiF–YF_3 melts is illustrated in Fig. 1 for the 45 mol% LiF–55 mol% YF_3 mixture. The melting and freezing reactions observed using the platinum crucibles give sharp, single peak profiles whereas dual reaction profiles were clearly observed when using tantalum crucibles. These effects can be attributed to the thermal lag which is a consequence of the wide distribution of the melt within the crucible and such effects mean that reliable melting or freezing temperatures cannot be obtained using tantalum crucibles. Indeed, double peaks of this kind could easily be wrongly attributed to a constitutional feature of the phase diagram.

The samples for EBS analysis were prepared by conventional metallographic techniques and

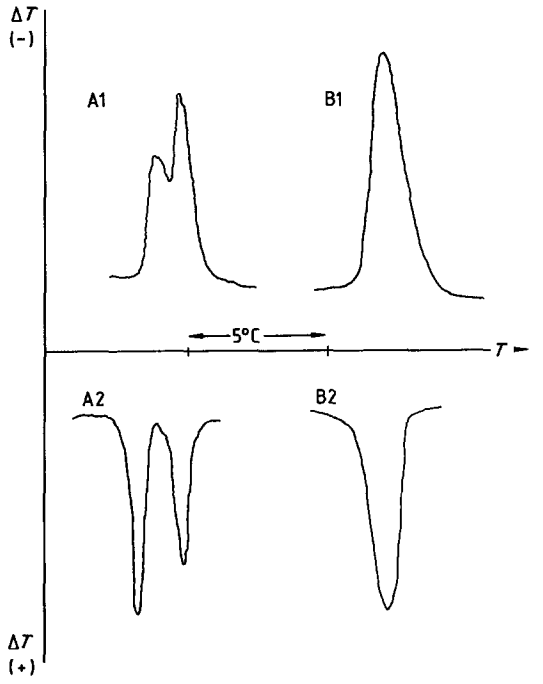

Figure 1 Melting and freezing reactions for a 45 mol% LiF–55 mol% YF_3 mixture. A1–melting reaction using a tantalum crucible; B1–melting reaction using a platinum crucible; A2–freezing reaction using a tantalum crucible; B2–freezing reaction using a platinum crucible. The vertical scale has arbitrary units, $\Delta T(+)$ and $\Delta T(-)$ represent respective heat emission and absorption during reaction.

because they are insulators, the polished surfaces of the samples were coated with a thin layer of carbon prior to examination in the SEM.

3. Experimental results and discussion

3.1. Crystallization behaviour during Czochralski growth

During Czochralski single crystal growth, significant differences in crystallization behaviour have been noted between $LiErF_4$, $LiLuF_4$ and $LiYF_4$. $LiErF_4$ and $LiLuF_4$ melts prepared from transparent portions of the zone-refined bars can be seeded readily whilst on occasions, corresponding $LiYF_4$ melts are seeded only with difficulty. The seed–melt interface for $LiErF_4$ and $LiLuF_4$ has the meniscus shape depicted in Fig. 2a and the melt in the meniscus region is optically clear: this behaviour is typical for the Czochralski growth of optically transparent compounds which either melt congruently or approximate closely thereto, as is the case for dilute solid solutions. For $LiYF_4$, the meniscus height is increased substantially at seed-on and during initial growth as illustrated

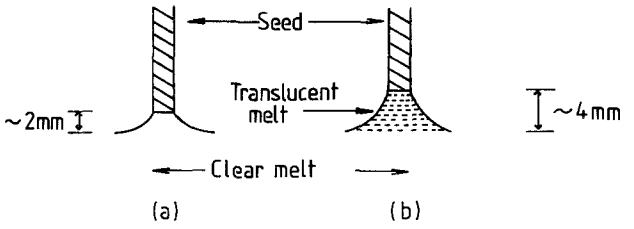

Figure 2 Meniscus conditions during seeding in Czochralski growth for stoichiometric melts of (a) $LiErF_4$ and $LiLuF_4$ and (b) $LiYF_4$.

in Fig. 2b, indicative of a higher surface tension, and the melt adjacent to the solidifying interface becomes semi-translucent, giving the impression that it contains fine particles in suspension. Single crystals of $LiYF_4$ can be grown under these conditions but the first material to crystallize, namely the crystal neck, is translucent and mechanically fragile. The translucent region often extends only for a few millimetres and consists of small clear crystallites surrounded by an opaque phase; X-ray powder diffractometry has established that this region contains the YF_3 phase in addition to $LiYF_4$ and suggests that the seeding problem is constitutional in origin. An identical effect has been observed in the single crystal growth of compounds related to $LiYF_4$, such as the $LiY_{0.5-x-y}Er_{0.5}Tm_xHo_yF_4$ series used in eye-safe laser applications [2], where it was shown that the addition of a small excess of LiF eliminated the seeding problem. Similar LiF additions made during the present work have also eliminated the seeding problem for $LiYF_4$ and restored the normal meniscus characteristics of Fig. 2a. If it is assumed that the transparent portions of zone-refined material correspond to a 1:1 mixture of $LiF:YF_3$, then a composition adjusted to 1.03:1 consistently gave good seeding.

Deliberate changes made to melt compositions within the $LiF:RF_3$ limits 1.12:1 to 1:1.06 for the three systems, established that transparent single crystals could be grown on both the LiF- and RF_3-rich sides of $LiRF_4$ for both $LiErF_4$ and $LiLuF_4$ but not for $LiYF_4$. For this compound, attempts to produce crystals from YF_3-rich melts always produced polycrystalline opaque material containing the YF_3 phase; crystals could, however, be grown consistently from melts within the $LiF:YF_3$ limits 1.12 to 1.03:1.

It must be emphasized that the crystal growth data described here applies only to preparative conditions where oxygen and water vapour have been rigorously excluded. These cause contamination [5–7] and mask the effects described.

The crystal growth data for $LiErF_4$ and $LiLuF_4$ are consistent with the presence of a compound at the 1:1 $LiF:RF_3$ composition which melts in a clearly defined congruent manner, otherwise growth from both LiF- and RF_3-rich melts would not be possible. The situation for $LiYF_4$ is less readily discerned. Because conditions for seeding and single crystal growth of $LiYF_4$ can be established for 1:1 compositions, albeit with difficulty, a close approximation to congruent melting behaviour is implied. However, the absence of suitable compositions for growth from slightly YF_3-rich melts whilst growth from very slightly LiF-rich melts is possible, could be explained by either peritectic or syntectic melting reactions (see later). Nevertheless, for growth to be possible at all, the compositions of the liquid components of such reactions must be very close indeed to that of the compound $LiYF_4$, otherwise segregation effects would preclude the production of optically transparent material. The changes noted in the meniscus behaviour of these melts would be consistent with either syntectic or peritectic behaviour [3, 4] since both could produce small volumes of two-phase material near to the solidification temperature. Despite these observations, the crystal growth evidence for the type of melting reaction in $LiYF_4$ is considered inconclusive because the changes observed occur within such narrow composition limits ($<$ 1.03:1 to 1:1) that small deliberate changes made to melt composition might be modified and therefore masked by either very small losses of the volatile component, LiF, or by very small changes in contamination by oxygen or water vapour; both of these factors have been shown to be important for $LiYF_4$ [2, 6, 7] although the volatility problem is controlled substantially in the experimental conditions used here [2]. The crystallization behaviour will be examined again in the light of the DTA studies.

3.2. DTA studies

In order to understand more clearly the crystal growth behaviour reported in the previous section, the phase diagrams of the $LiF–LuF_3$, $LiF–ErF_3$

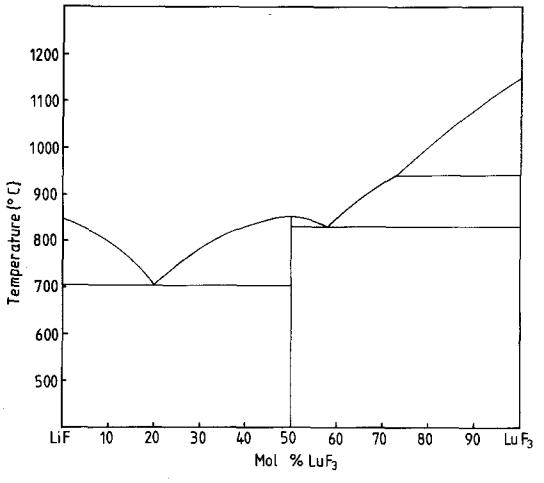

Figure 3 The $LiF-LuF_3$ phase diagram.

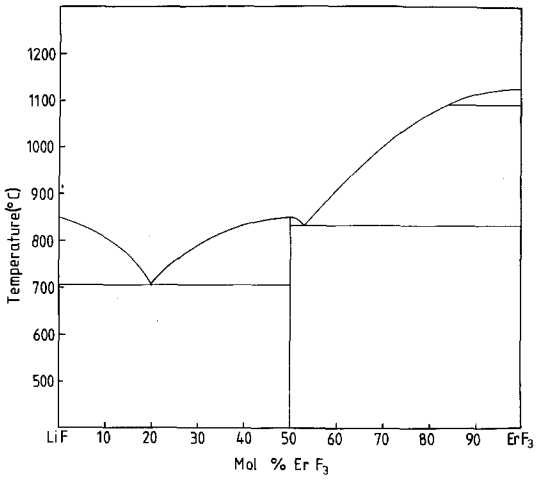

Figure 4 The $LiF-ErF_3$ phase diagram. Includes data from [6].

and $LiF-YF_3$ have been determined by DTA measurements, with particular attention being paid to the region of the phase diagrams around the 50/50 composition.

3.2.1. The $LiF-LuF_3$ system

The $LiF-LuF_3$ phase diagram determined in this investigation is shown in Fig. 3 and the data were obtained using tantalum crucibles. Selected compositions were also examined using platinum crucibles and good agreement between the two sets of results was obtained.

Fig. 3 shows clearly that the phase $LiLuF_4$ is congruent in nature with a melting point of $850 \pm 3°$ C. The main features of the phase diagram are summarized in Table I together with some previously reported data [4]. There are significant differences between the two sets of data in terms of the melting points of the $LiLuF_4$ phase, the temperatures of the high and low temperature eutectic reactions and the composition of the $LiF-LiLuF_4$ eutectic mixture. There is good agreement between the compositions of the $LiLuF_4-LuF_3$ eutectic mixture and the temperatures of the solid-state reaction in LuF_3.

Reproducible DTA data were obtained even after a number of heating and cooling cycles, thus indicating the absence of any significant contamination in this system. The crystal growth characteristics of the $LiLuF_4$ compound reported earlier are completely consistent with the phase diagram shown in Fig. 3.

3.2.2. The $LiF-ErF_3$ system

The $LiF-ErF_3$ phase diagram determined in this work is shown in Fig. 4, the data being obtained using tantalum (and platinum) crucibles.

The phase $LiErF_4$ is clearly congruent with a melting point of $850 \pm 3°$ C which, within experimental limits, is identical with that of $LiLuF_4$. This observation is in contrast to that of Thoma

TABLE I

System	$LiF-YF_3$		$LiF-LuF_3$		$LiF-ErF_3$	
	Present work	Thoma *et al.* [3]	Present work	Thoma [4]	Present work	Thoma [4]
Composition of $LiF-LiRF_4$ eutectic (mol %)	80–20	80–20	80–20	70–30	80–20	70–30
Temperature of $LiF-LiRF_4$ eutectic (° C)	706 ± 2	~ 690	704 ± 2	~ 680	706 ± 2	~ 660
Composition of $LiRF_4-RF_3$ eutectic (mol %)	49–51	Shown as a peritectic	42–58	42–58	47–53	42–58
Temperature of $LiRF_4-RF_3$ eutectic (° C)	830 ± 2	–	832 ± 2	~ 780	831 ± 2	~ 800
Melting temperature of $LiRF_4$ compound (° C)	830 ± 2	~ 825 (Peritectic)	850 ± 3	~ 795	850 ± 3	~ 825

et al. [4] who indicated a melting point for $LiLuF_4$ significantly lower than that of $LiErF_4$. The present result is in very good agreement with our previous DTA studies on $LiErF_4$ [6]. The main features of the $LiF-ErF_3$ phase diagram are summarized in Table I together with some previously reported data [4]. As in the case of the $LiF-LuF_3$ system, the temperatures of the various reactions are all higher in the present work and the composition of the $LiF-LiErF_4$ eutectic mixture is at 20 mol % ErF_3 rather than 30 mol % ErF_3 [4].

Cycling experiments again indicated the absence of significant contamination effects in this system and the previously described crystal growth characteristics of $LiErF_4$ are completely consistent with the phase diagram shown in Fig. 4.

3.2.3. The $LiF-YF_3$ system

The $LiF-YF_3$ phase diagram is shown in Fig. 5, the DTA data being obtained using platinum crucibles only. The main features of the diagram are summarized in Table I together with some previously reported data [3]. Identification of the $LiYF_4/YF_3$ eutectic composition by DTA measurement alone was not possible and the eutectic composition at 51 mol % YF_3 was derived from the microstructural studies discussed later. The present work differs from previous studies by showing that $LiYF_4$ is either just congruent or possibly syntectic in nature with a melting reaction at 830 ± 2° C rather than peritectic with a melting reaction at 825° C. The temperature of 830° C for the melting reaction is in very good agreement with that reported in [5, 6]. The difficulties in resolving the very small temperature differences in this system by DTA alone are illustrated by the inability to detect a eutectic/liquidus separation between $LiYF_4$ and the $LiYF_4/YF_3$ eutectic which should be present for both congruent and syntectic reactions. On occasions, the formation of two spheres has been noted after solidification of the 50/50 DTA samples which suggests liquid immiscibility and would be consistent with a syntectic reaction.

Thermal cycling confirms the reactive nature of $LiYF_4$ since the appearance of the $LiF/LiYF_4$ eutectic reaction after the initial heating run in hyperstoichiometric compositions is consistent with contamination observed during deliberate oxidation experiments [7].

The present studies are in general agreement with our previous observations on zone refined material and with certain aspects of our suggested phase diagram for the $LiF-YF_3$ system [6]. They are also in agreement with the crystal growth studies of Pastor *et al.* [8]. All these studies showed that, providing contamination was avoided, then a congruent melting reaction could be obtained for $LiYF_4$.

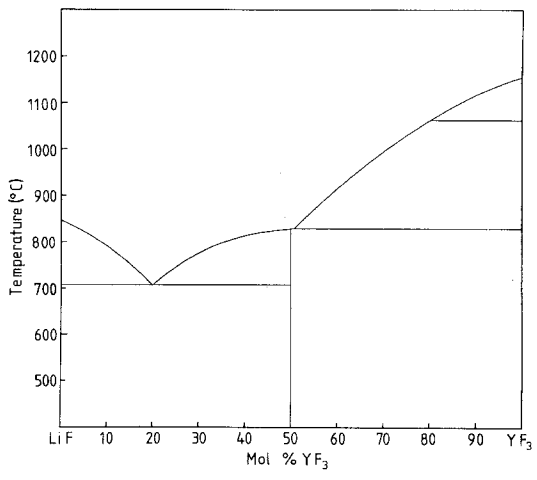

Figure 5 The $LiF-YF_3$ phase diagram. The region between 50 and 51 mol % YF_3 can only be represented as a single line because of the extremely narrow (and hence unresolved) liquidus/eutectic separation in this region. The presence of the eutectic at 51 mol % YF_3 is clearly indicated by the microstructural studies (see Fig. 6c).

3.3. Microstructural studies

The microstructures of the various compositions are revealed clearly in the SEM by EBS where differences in contrast are derived from the average atomic number of the phases present. The systems investigated here are particularly advantageous because of the large mean atomic number variations which occur.

The microstructures of the 57 mol % YF_3 and 55 mol % YF_3 samples (Figs. 6a and b) exhibit dendrites of the primary YF_3 phase with a fine eutectic ($YF_3 + LiYF_4$) in-filling which is entirely consistent with Fig. 5. The microstructure of the 51 mol % YF_3 sample (Fig. 6c) consists entirely of a eutectic mixture, the eutectic mixture being characteristically thread-like. This observation has been used to fix the $YF_3/LiYF_4$ eutectic composition in Fig. 5. Fig. 6d shows a region of the 50 mol % YF_3 sample (the $LiYF_4$ composition) which consists of a mixture of the $LiYF_4$ phase with eutectic in-filling. The microstructure of the 48 mol % YF_3 sample is shown in Fig. 6e and

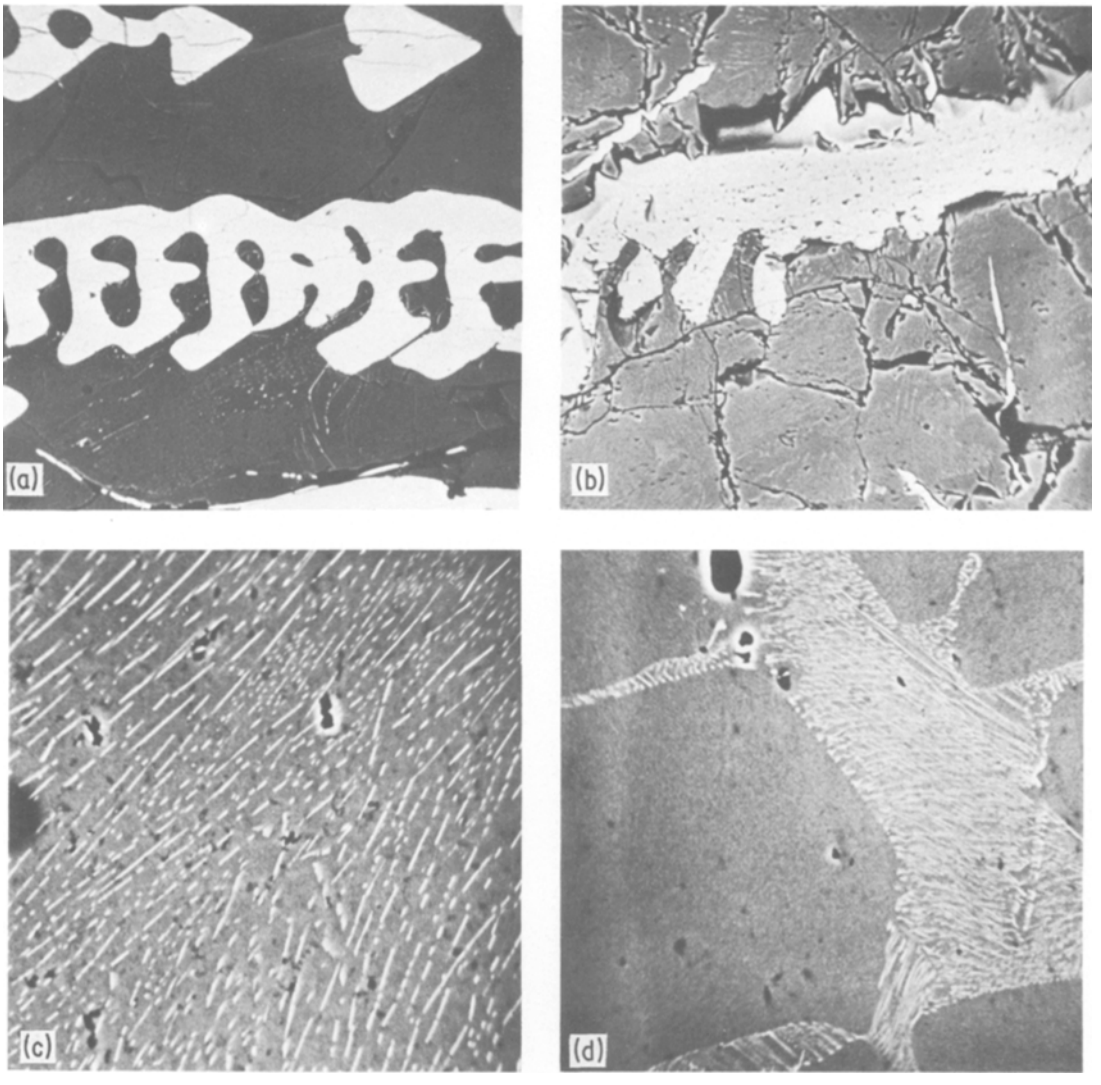

Figure 6 EBS micrographs of LiF–RF_3 mixtures. (a) 43 mol% LiF: 57 mol% YF_3, (×100). The very fine $LiYF_4/YF_3$ eutectic can just be observed between the primary YF_3 dendrites. (b) 45 mol% LiF: 55 mol % YF_3, (×200). This sample is extensively cracked and hence the crazed appearance. The very fine eutectic mixture can just be seen in the background. (c) 49 mol% LiF: 51 mol% YF_3, (×500). This fine $LiYF_4/YF_3$ eutectic mixture is characteristic of the whole sample. (d) 50 mol% LiF: 50 mol% YF_3, (×500). This shows a region of the sample which consists of primary $LiYF_4$ together with the $LiYF_4/YF_3$ eutectic mixture. (e) 52 mol% LiF: 48 mol% YF_3, (×200). This microstructure consists of primary $LiYF_4$ together with the $LiF/LiYF_4$ and $LiYF_4/YF_3$ eutectic mixtures in close association with one another. (f) 80 mol% LiF: 20 mol% YF_3, (×320). The $LiF/LiYF_4$ rod-like eutectic with some primary LiF (dark phase). (g) 80 mol% LiF: 20 mol% ErF_3, (×320). Rod-like $LiF/LiErF_4$ eutectic mixture with no evidence of any primary phase. (h) 80 mol% LiF: 20 mol% LuF_3 (×320). Rod–like $LiF/LiLuF_4$ eutectic mixture with no primary phase.

consists of a mixture of the $LiYF_4$ phase together with the $LiF/LiYF_4$ and the $YF_3/LiYF_4$ eutectic mixtures in close association with each other.

The presence of the higher temperature eutectic both in the 50/50 sample and particularly in the 48 mol% YF_3 sample, where an intimate mixture of both the high and low temperature eutectics is observed, can be explained by a syntectic reaction of the type shown schematically in Fig. 7, if freezing occurs under non-equilibrium conditions.

The microstructure of the 20 mol% YF_3 sample shown in Fig. 6f is predominantly eutectic in nature, in reasonable agreement with the phase diagram of Fig. 5. The eutectic is rod-like in

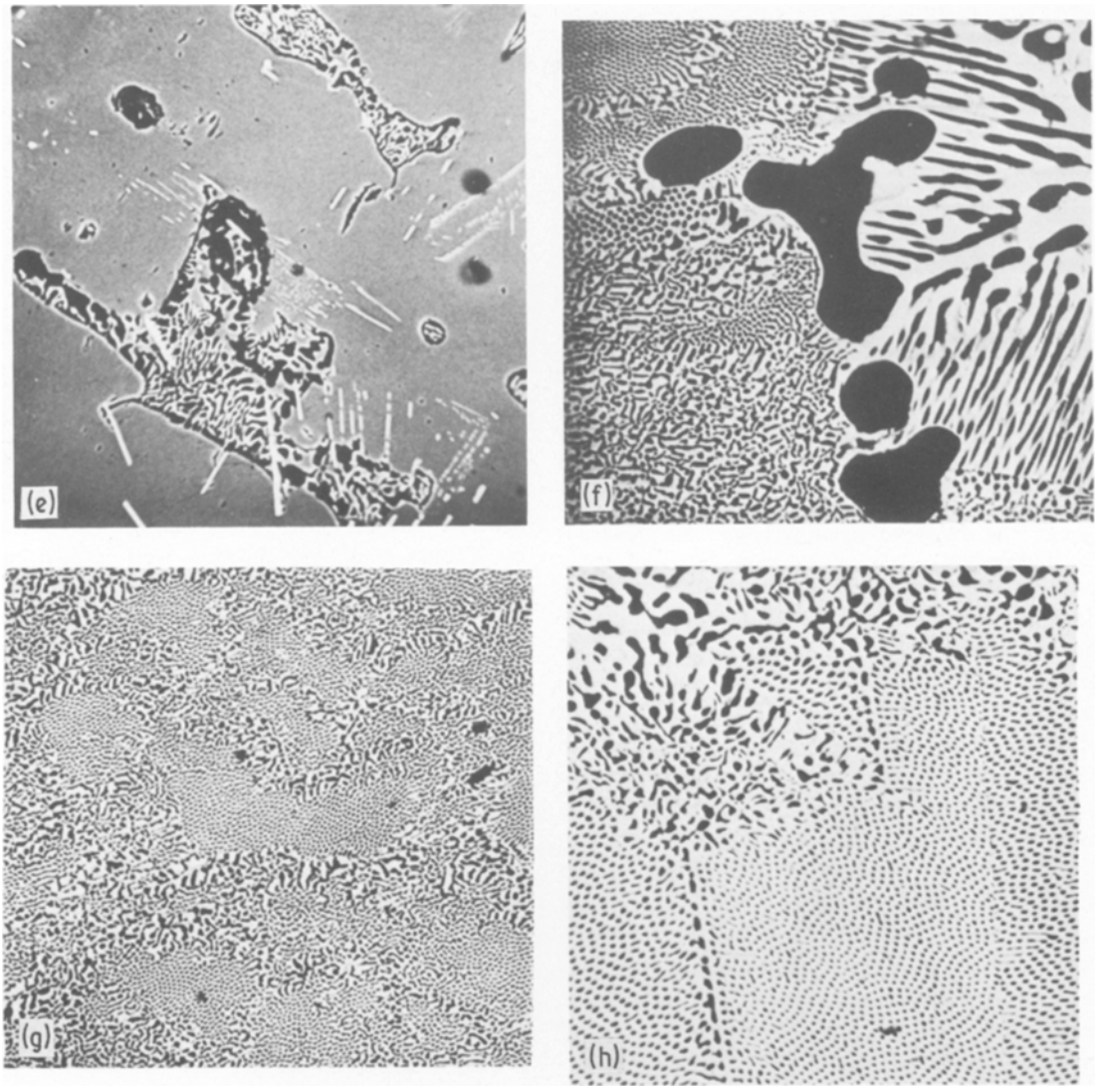

Figure 6 Continued.

character and of similar morphology to the 20 mol % ErF_3 (Fig. 6g) and 20 mol % LuF_3 (Fig. 6h) eutectic samples.

Detailed microstructural studies have also been carried out on a selection of samples from the LiF–ErF_3 and LiF–LuF_3 systems and these studies confirm the general features of the phase diagrams shown in Figs. 3 and 4.

4. Discussion of the constitutional aspects of the LiF–YF_3 system

The LiF–YF_3 phase diagram reported here is completely consistent with the crystal growth characteristics described in Section 3.2.1. A syntectic reaction at the 50/50 composition would lead to immiscible liquids and explain both the "seeding-on" difficulties and the removal of this effect by the addition of a small amount of excess LiF. The failure to grow transparent single crystals of $LiYF_4$ on the YF_3-rich side of the stoichiometric composition can also be explained in terms of the syntectic reaction and the close proximity of the $LiYF_4/YF_3$ eutectic to the 50/50 composition. A syntectic reaction at the 50/50 composition would explain why the translucent neck of Czochralski-grown crystals contains YF_3 because this would necessarily be associated with the higher melting point eutectic. The fact that the "seeding-on" problem did not occur everytime and that it was possible to produce good, clear,

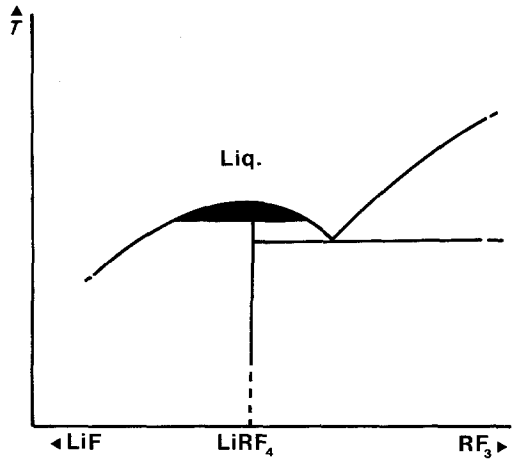

Figure 7 A schematic representation of a possible syntectic reaction for the solidification of an $LiRF_4$ compound. The blackened region represents the immiscible liquid phase field.

single crystals of $LiYF_4$ from a starting charge of the zone-refined material [5], suggests that congruent melting is the normal state and that the "seeding-on" problem, when it occurs, is the result of slight contamination during melt preparation which changes the very critical freezing reaction in this system from congruent to syntectic with a narrow liquidus/syntectic temperature separation.

The work of Pastor *et al.* [8] would support this view as they indicated a $LiYF_4/YF_3$ eutectic composition of 56 mol% YF_3 for material produced entirely in HF compared with 51 mol% YF_3 seen in the present work. This shift in the eutectic composition could indicate a slightly higher level of purity for materials produced solely in HF.

In earlier discussion [5], a homogeneity range for the $LiYF_4$ phase was invoked in order to explain some of the DTA profiles. The phase relationships determined here show little evidence of an extensive homogeneity range, although a limited range must exist in order to explain observed retrograde solid solubility effects [2]. The melting behaviour reported previously [5] can be explained by the proposed syntectic reaction. From a practical viewpoint it should be noted that the growth characteristics of $LiYF_4$ are very similar to those of the α/β-LYF crystals used as solid-state lasers and that the growth techniques used herein have yielded consistently good quality laser material. Hence, although a total HF system of the type employed by Pastor *et al.* [8] gives unequivocal congruent melting behaviour, it is not an essential prerequisite for device production.

5. General discussion of the constitutional aspects of $LiF-RF_3$ systems

The composition of the LiF/RF_3 eutectic for the $LiF-ErF_3$ and $LiF-LuF_3$ systems is at significantly higher LiF composition than that observed previously. In addition the temperatures of the eutectics for all three systems are significantly higher than the previously reported values (see Table I). These observations, together with the higher melting points of the $LiRF_4$ phases, are all consistent with the greater stability of these phases which is derived principally from a lower level of contamination in the present work.

There is other evidence in the literature to support the dependence of the stability of the $LiRF_4$-type phases on their impurity content. For instance, the $LiF-YbF_3$ phase diagram determined by Thoma *et al.* [4] shows a well defined congruent melting reaction at 800° C for the $LiYbF_4$ phase, the phase being stable down to room temperature, whereas Bukhalova *et al.* [9] show a peritectoid reaction whereby $LiYbF_4$ dissociates to LiF and YbF_3 on heating to 586° C. These profound differences in the stability of the $LiYbF_4$ phase could be due to the different purities of the materials used. The present work suggests that the material employed by Bukhalova *et al.* [9] was less pure.

The DTA data summarized in Table I emphasize that the purer the starting materials and the DTA environment, the higher are the melting points of the $LiRF_4$ phases. In the light of the present and previous work therefore, it can be suggested that, in the $LiF-RF_3$ systems, the melting behaviour can undergo the transitions congruent → syntectic → peritectic → peritectoid as the level of contamination is increased. Such an effect superimposed on the normal changes in $LiRF_4$ compound stability expected to occur as the size of the R ion is changed would undoubtedly lead to much of the confusion about melting behaviour which has existed hitherto.

6. Conclusions

The crystal growth, DTA and microstructural studies carried out in the present work have shown that:

(i) The phases $LiLuF_4$ and $LiErF_4$ are congruent in nature and their melting points are significantly higher than the previously reported values.

(ii) The compositions of the $LiF-LiLuF_4$ and $LiF-LiErF_4$ eutectics are at significantly higher

LiF-contents (80 mol% LiF) than those previously reported.

(iii) The phase $LiYF_4$ is either just congruent or just syntectic in nature, depending upon the level of contamination, an observation in major disagreement with the previously published phase diagram which shows a clearly defined peritectic reaction.

Acknowledgements

This work was carried out with the support of Procurement Executive, Ministry of Defence. Thanks are due to Dr G. T. Brown of RSRE, Malvern for useful discussions.

References

1. E. P. CHICKLIS, C. S. NAIMAN, R. C. FOLWEILER, D. R. GABBE, H. P. JENSSEN and A. LINZ, *Appl. Phys. Lett.* **19** (1971) 119.
2. B. COCKAYNE, J. G. PLANT and R. A. CLAY, *J. Cryst. Growth* **54** (1981) 407.
3. R. E. THOMA, C. F. WEAVER, H. A. FRIEDMAN, H. INSLEY, L. A. HARRIS and H. A. YAKEL, *J. Phys. Chem.* **65** (1961) 1096.
4. R. E. THOMA, *Prog. Sci. Tech. Rare Earths* **2** (1966) 110.
5. J. S. ABELL, I. R. HARRIS, B. COCKAYNE and J. G. PLANT, *J. Mater. Sci.* **11** (1976) 1807.
6. J. S. ABELL, I. R. HARRIS and B. COCKAYNE, *ibid.* **12** (1977) 670.
7. H. SAFI, I. R. HARRIS, B. COCKAYNE and J. G. PLANT, *ibid.* **16** (1981) 3203.
8. R. C. PASTOR, M. ROBINSON and W. M. AKUTAGAWA, *Mater. Res. Bull.* **10** (1975) 501.
9. G. A. BUKHALOVA and E. P. BABAEVA, *Russ. J. Inorg. Chem.* (English translation) (1966) 339.

Received 31 August
and accepted 20 September 1982